Mechanical Systems and Signal Processing ▮ (▮▮▮▮) ▮▮▮–▮▮▮

Contents lists available at ScienceDirect

Mechanical Systems and Signal Processing

journal homepage: www.elsevier.com/locate/jnlabr/ymssp

Combined MIMO adaptive and decentralized controllers for broadband active noise and vibration control

A.P. Berkhoff [a,b,*], J.M. Wesselink [b]

[a] TNO Science and Industry, MON-Acoustics, PO Box 155, 2600AD Delft, The Netherlands
[b] University of Twente, EEMCS-Signals and Systems, PO Box 217, 7500AE Enschede, The Netherlands

ARTICLE INFO

Article history:
Received 11 May 2010
Received in revised form
13 September 2010
Accepted 21 December 2010

Keywords:
Active noise and vibration control
Adaptive algorithms
HAC/LAC
Decentralized control

ABSTRACT

Model errors in multiple-input multiple-output adaptive controllers for reduction of broadband noise and vibrations may lead to unstable systems or increased error signals. In this paper, a combination of high-authority control (HAC) and low-authority control (LAC) is considered for improved performance in case of such model errors. A digital implementation of a control system is presented in which the HAC (adaptive MIMO control) is implemented on a CPU and in which the LAC (decentralized control) is implemented on a high-speed Field Programmable Gate Array. Experimental results are given which demonstrate that the HAC/LAC combination leads to performance advantages in terms of stabilization under parametric uncertainties and reduction of the error signal.

1. Introduction

Many algorithms used for broadband active noise control are based on the adaptive Least Mean Square (LMS) algorithm [1]. The low complexity and the relatively good robustness properties are the major advantages of the LMS algorithm. Recent algorithms solve many of the problems associated with the speed of convergence of the older algorithms. The basis for a particular class of such algorithms has been given by Elliott [2] as the preconditioned LMS algorithm. The version based on the filtered-error algorithm [3] is more efficient for multiple reference signals than the filtered-reference algorithm. A proper implementation of the filtered-error preconditioned LMS algorithm solves many of the problems associated with early implementations of the LMS algorithm, such as slow convergence due to frequency dependence of the secondary path and cross-coupling in the secondary path [4]. However, the controller is model-based and is, therefore, still sensitive for mismatch between the model and the plant. This model mismatch reduces the overall performance of the controller. Model mismatch can be caused by variations in parameters such as temperature, boundary conditions, etc. For some control schemes, online adaptation of the model is possible in principle but a large amount of additional noise has to be injected in the system for rapid changes in the model [5]. Furthermore, if the controller uses model-based preconditioning or factorization, then these time-consuming operations should be performed online as well. Robust control approaches are known [6] as well as probabilistic methods leading to frequency-dependent regularization for optimum filtering [7,8] and adaptive control [9,10]. Such algorithms can be tuned for a particular application but require additional effort in the design stage and presume that sufficient a-priori knowledge is available about the uncertainty. An alternative approach is to use a high-authority and low-authority control (HAC/LAC) architecture [11], where the goal

* Corresponding author at: TNO Science and Industry, MON-Acoustics, PO Box 155, 2600AD Delft, The Netherlands.
E-mail addresses: a.p.berkhoff@utwente.nl, arthur.berkhoff@tno.nl (A.P. Berkhoff).

0888-3270/$ - see front matter © 2011 Elsevier Ltd. All rights reserved.
doi:10.1016/j.ymssp.2010.12.012

of the low-authority controller is to add active damping to the structure. Active damping can be implemented using different strategies. The use of a HAC/LAC architecture yields three major advantages [11]. Firstly, the active damping extends outside the bandwidth of the HAC control loop, which reduces the settling times outside the control bandwidth. Secondly, it is easier to gain-stabilize the modes outside the bandwidth of the outer loop. And thirdly, the large damping of the modes inside the controller bandwidth makes them more robust to parametric uncertainty. In the paper by Herold et al. [12], a method using piezoelectric sensors and actuators and positive position feedback(PPF) was described. In the PPF-method, a second-order filter is used as the control filter which is combined with positive feedback. The control filter is then tuned to reduce one of the desired resonance peaks.

In the present paper, an approximately collocated and dual sensor–actuator pair is used, suitable for broadband damping as described by Elliott et al. [13]. If the actuator–sensor system is dual and collocated, a simple decentralized proportional feedback controller is sufficient to add damping due to the fact that the overall energy that is stored in the system will be reduced [11]. As such, less detailed a-priori information is required about the model uncertainty. Active damping is not very effective for frequencies that do not coincide with the poles and zeros. To gain further reductions for such frequency components a model-based controller is used such as the RMFeLMS algorithm as described in this paper. Section 2 gives a description of the panel, the control architecture, the control hardware and the particular implementation

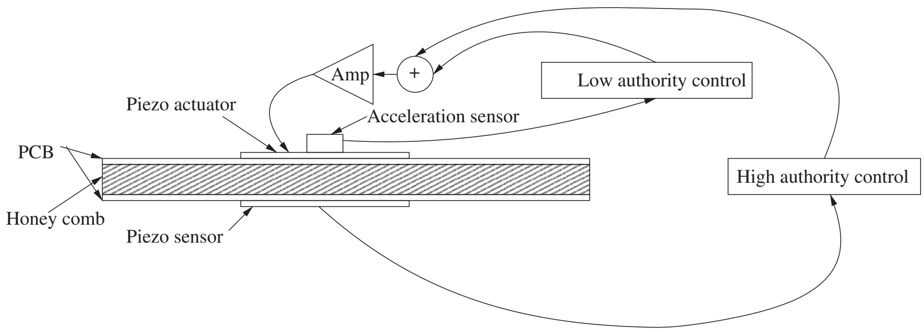

Fig. 1. Configuration of the high-authority/low-authority control architecture applied to a sandwich panel with piezoelectric patch actuators, piezoelectric patch sensors and accelerometers.

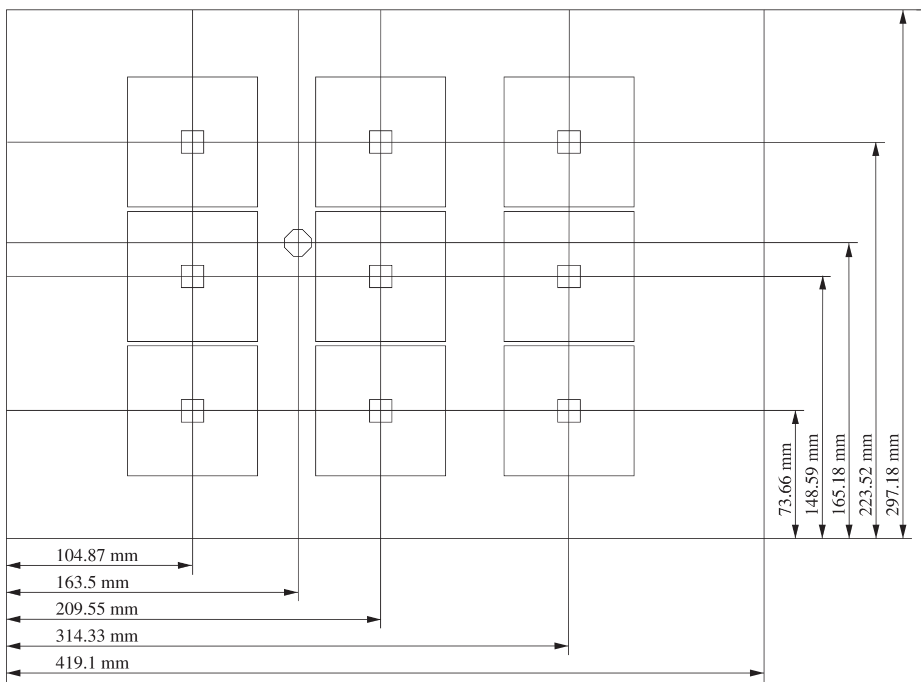

Fig. 2. Dimensions of the active panel used in the experiments. A mount with a thread was used to attach extra weight to the panel (indicated by a circle).

Please cite this article as: A.P. Berkhoff, J.M. Wesselink, Combined MIMO adaptive and decentralized controllers for broadband active noise and vibration control, Mechanical Systems and Signal Processing (2011), doi:10.1016/j.ymssp.2010.12.012

of the adaptive MIMO control algorithm. Section 3 presents the results on the design of the decentralized feedback loops and the combination of decentralized feedback with adaptive MIMO control. Results are given for the speed of convergence, reduction of the mean-squared error and the robustness of the system.

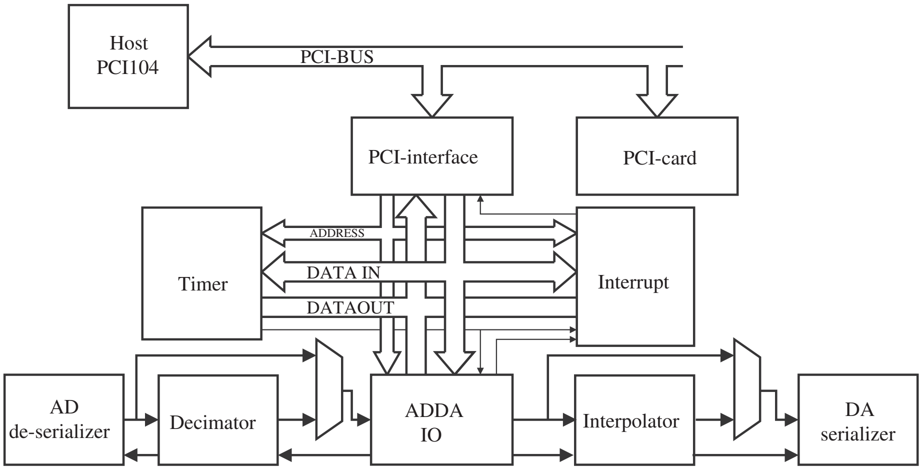

Fig. 3. Architecture of the FPGA (without the LAC unit).

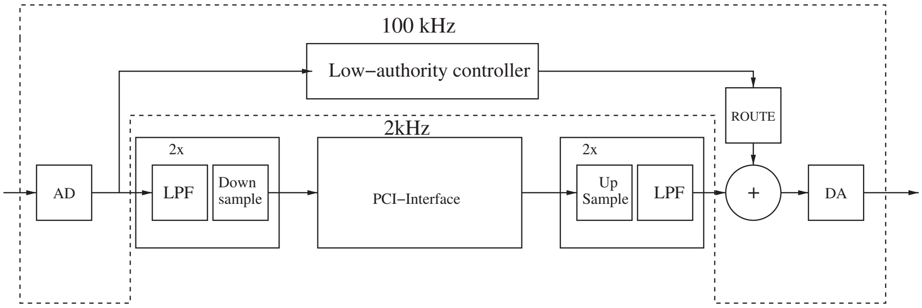

Fig. 4. Simplified block diagram of the control system containing the low-authority controller and down-/upsampling for the high-authority controller.

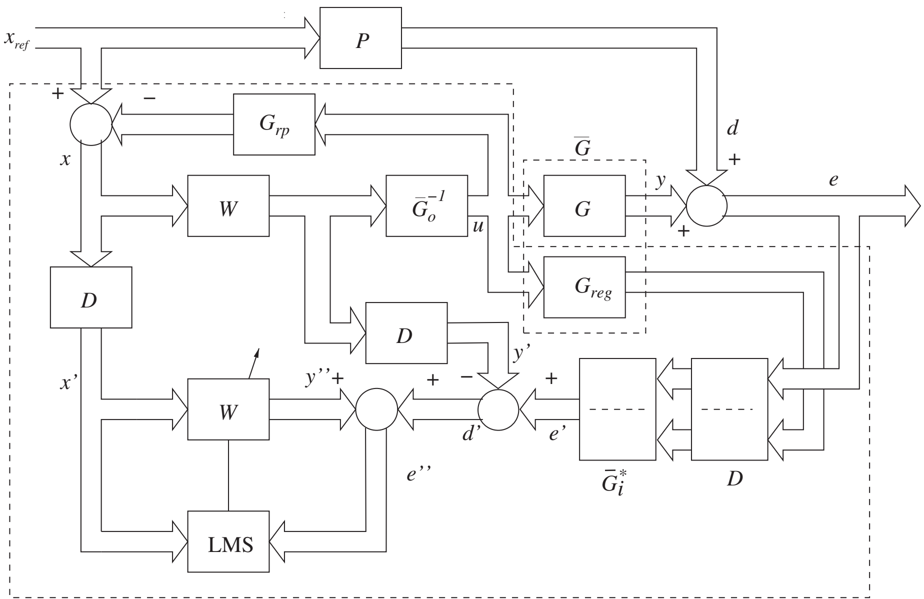

Fig. 5. Regularized modified filtered-error adaptive control scheme with IMC [14,4].

Please cite this article as: A.P. Berkhoff, J.M. Wesselink, Combined MIMO adaptive and decentralized controllers for broadband active noise and vibration control, Mechanical Systems and Signal Processing (2011), doi:10.1016/j.ymssp.2010.12.012

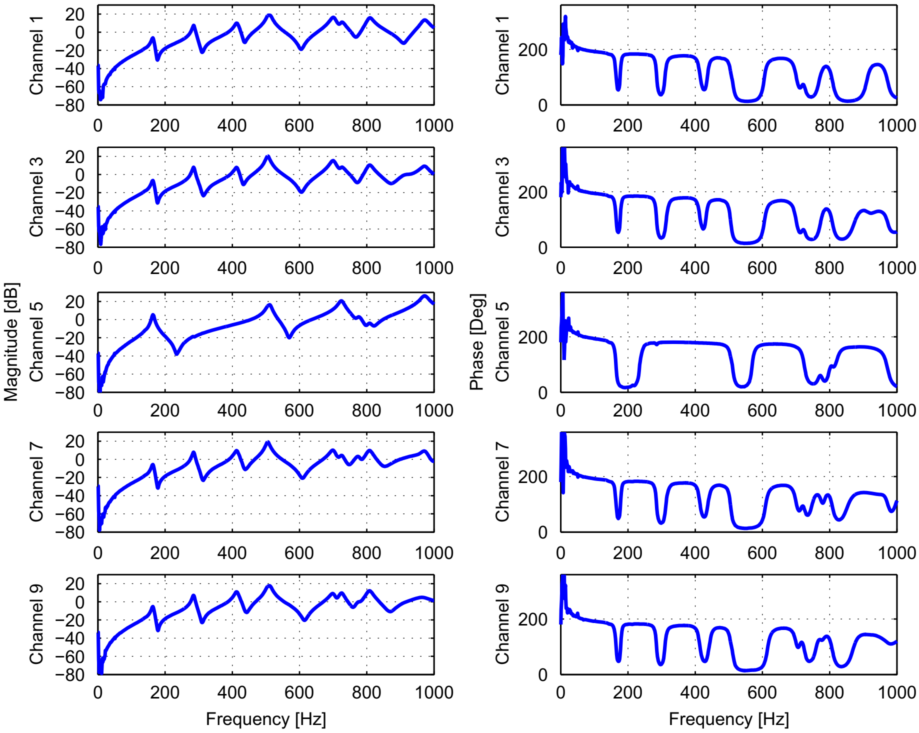

Fig. 6. The transfer functions for the collocated sensor–actuator pairs from 0 to 1 kHz; piezoelectric actuator to acceleration sensor, five pairs of the available nine pairs were used.

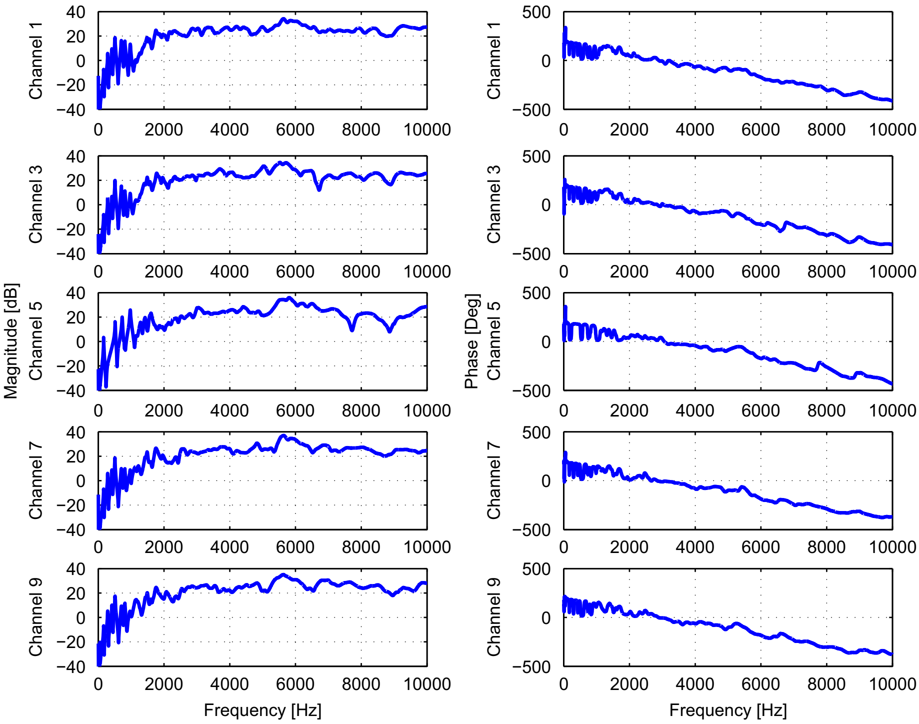

Fig. 7. As Fig. 6, except for the frequency range being 0–10 kHz.

Please cite this article as: A.P. Berkhoff, J.M. Wesselink, Combined MIMO adaptive and decentralized controllers for broadband active noise and vibration control, Mechanical Systems and Signal Processing (2011), doi:10.1016/j.ymssp.2010.12.012

2. Methods

In this paper, a particular implementation a MIMO adaptive algorithm (HAC) is combined with a decentralized feedback controller (LAC). The implementation of the adaptive algorithm uses the inverse of the minimum-phase factor of the secondary path, combined with a double set of control filters to eliminate the negative effect of the delay in the adaptation loop [14]. The latter algorithm is combined with a regularization technique that preserves the factorization properties [14]. The secondary path is estimated using subspace identification techniques [15]. This enables the use of reliable numerical techniques for the minimum-phase/all-pass decomposition using inner–outer factorization [16,17]. The resulting

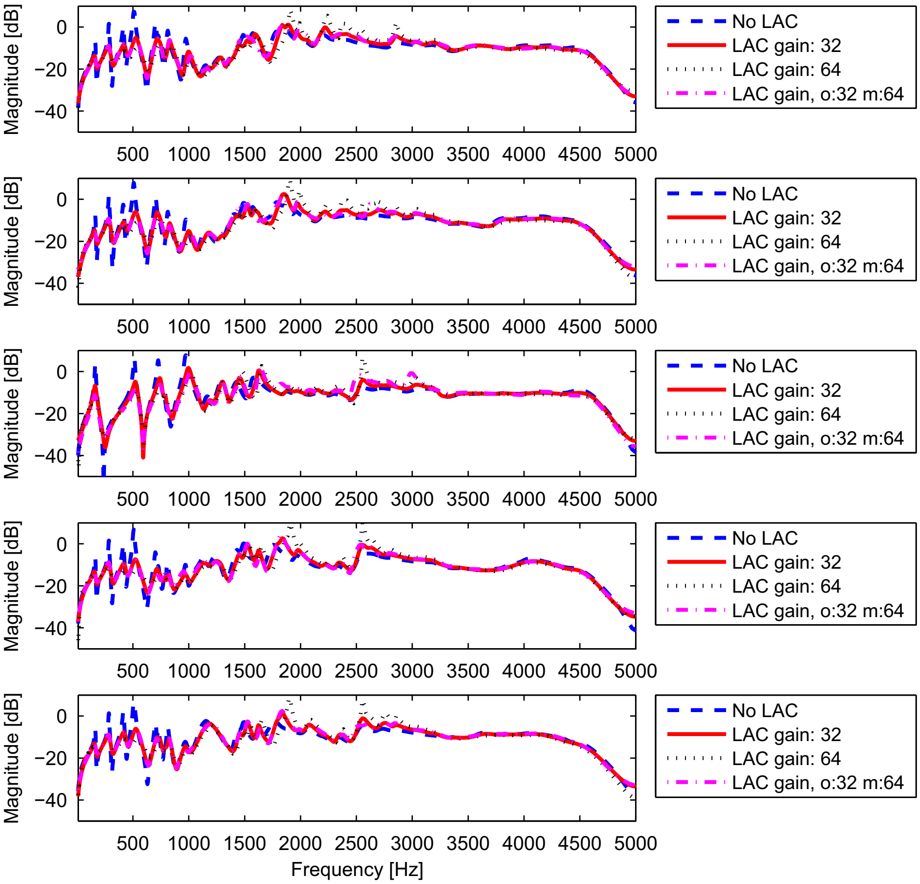

Fig. 8. Influence of low-authority controller on the transfer function of the plant, as measured from the piezoelectric actuator to the piezoelectric sensor, while the feedback loop was from the piezoelectric actuator to the acceleration sensor. The decimation filter was switched off; an interpolation filter with a stopband attenuation of 50 dB was used.

Table 1
Reduction of the error signals for a feedback controller for different step sizes α after 60 s.

α	$\frac{1}{10}$	$\frac{1}{20}$	$\frac{1}{40}$	$\frac{1}{80}$	$\frac{1}{160}$	$\frac{1}{320}$
MSE reduction (dB)	7.8	9.0	9.4	9.3	9.0	8.4

Table 2
Reduction of the error signals for a feedforward controller using different step sizes α after 60 s.

α	1	$\frac{1}{2}$	$\frac{1}{5}$	$\frac{1}{10}$	$\frac{1}{20}$	$\frac{1}{40}$	$\frac{1}{80}$
MSE reduction (dB)	19.4	21.2	22.1	22.3	22.4	22.6	21.8

Please cite this article as: A.P. Berkhoff, J.M. Wesselink, Combined MIMO adaptive and decentralized controllers for broadband active noise and vibration control, Mechanical Systems and Signal Processing (2011), doi:10.1016/j.ymssp.2010.12.012

algorithm, the so-called regularized modified filtered-error least mean square algorithm (RMFeLMS) has good convergence properties as compared to the standard filtered-reference and filtered-error algorithm [4].

The HAC/LAC architecture was tested on a panel with piezoelectric transducers for the reduction of noise transmission, a cross-section of which can be found in Fig. 1. The dimensions of the panel and the positions of the actuators and the sensors are given in Fig. 2. The height and the width of the piezoelectric actuators and the sensors are both 76 mm; the thickness is 0.5 mm. Nine piezoelectric patch actuators and nine piezoelectric patch sensors were attached to the panel [4], of which the middle pair and the four pairs in the corners were used. The panel was built from two Printed Circuit Boards (PCBs) with a honeycomb layer in between. One advantage of this approach is that electronics can be integrated. Another advantage is that the actuator and the sensor can be placed on different faces of the panel, which improves the control of the acoustically relevant out-of-plane vibrations because the in-plane coupling between the actuator and the sensor is reduced [18]. Five collocated accelerometers were used for active damping with decentralized control using the piezoelectric patch actuators. The control results were obtained with a perspex box on which the panel was mounted. Inside this perspex box, noise was created with a loudspeaker which led to vibrations of the panel [4]. It is noted that large reductions of the error signals may lead to pinning of the control locations and thus to the formation of a new boundary condition yielding additional resonances at higher frequencies in the sound transmission spectrum [13]. These new resonances may cause an increase in the transmitted sound. Noise reductions for a similar panel can be found in Ref. [4].

Active damping is often realized using an analog controller [19–21]. One of the advantages of an analog controller is its low delay when compared to a digital controller. In this paper, a digital controller with a high-sample rate is used, such that the analog and digital controllers have identical performance for frequencies within the control bandwidth. The dedicated analog interface board was developed containing ADDA converters operating at a relatively high-sample rate (in this case 100 kHz). The lower sample rate was derived from the high-sample rate by downsampling. This made it possible to run the LAC and HAC controller at different sample rates, i.e., 100 and 2 kHz, respectively. The interface between the PCI-104 system running the HAC algorithm and the ADDA unit was implemented in reconfigurable hardware, in this case a Field Programmable Gate Array (FPGA), (see Fig. 3). The FPGA incorporates the following functional units: the decimation filters, the interpolation filters, the glue logic for the PCI bus interface and the low-authority controller (Fig. 4). The decimation filters and the interpolation filters were designed in such a way that the desired compromise between group-delay, filter transition band characteristics and stopband attenuation was obtained.

A block diagram of the multiple-input multiple-output adaptive controller as used for the high-authority controller is shown in Fig. 5. A detailed description of this algorithm can be found in Refs. [14,4]. Relevant for the experiments as

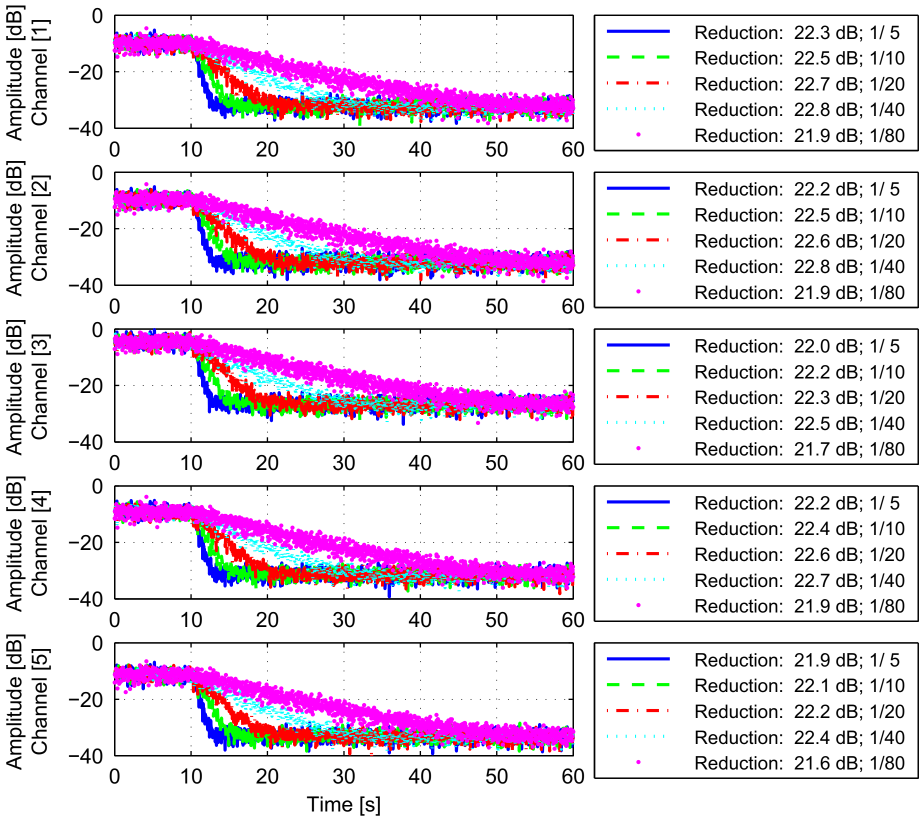

Fig. 9. Convergence curves for different α's using a feedforward controller. The format in the legend is: Reduction in dB; step size α.

described in this paper are the definition of the update rule for the controller and the regularization of the secondary path. For the description of the MIMO controller, we assume that there are K reference signals, L error sensors and M actuators. Denoting n as the sample instant, the update rule for the controller coefficients is

$$W_i(n+1) = W_i(n) - \alpha e''(n) x'^T(n-i), \tag{1}$$

where the i-th set of coefficients of the control filters are represented by the $M \times K$ matrix W_i, where $i = 0 \ldots N_W - 1$, i.e., $W(q) = \sum_{i=0}^{N_W-1} q^{-i} W_i$, where q is the unit delay operator. Furthermore, $e''(n)$ is the $M \times 1$ vector of auxiliary error signals, $x'(n)$ is the $K \times 1$ vector of delayed reference signals, and α is the convergence coefficient. In the actual implementation, a normalized LMS update rule was used, combined with 'leakage' of the control coefficients [10].

The regularization was implemented by defining an augmented plant $\overline{G}(q)$:

$$\overline{G}(q) = \begin{bmatrix} G(q) \\ G_{\text{reg}}(q) \end{bmatrix}, \tag{2}$$

in which the $L \times M$-dimensional secondary path $G(q)$ is augmented with an $L' \times M$-dimensional transfer function $G_{\text{reg}}(q)$. For the implementation as described in this paper, the regularization was based on a simple weighting of the $M \times 1$ vector of control signals $u(n)$, which also limits the inversion of zeros in $G(q)$ that are close to the unit circle, resulting in more stable behavior of the $M \times M$-dimensional inverse $\overline{G}_o(q)^{-1}$. The regularizing transfer function $G_{\text{reg}}(q)$ was defined as

$$G_{\text{reg}}(q) = \sqrt{\beta} I_M, \tag{3}$$

in which β is a scalar quantity and in which I_M is an $M \times M$ identity matrix. The all-pass factor $\overline{G}_i$ and the minimum-phase factor $\overline{G}_o$ are obtained from an inner–outer factorization such that $\overline{G} = \overline{G}_i \overline{G}_o$. The adjoint $\overline{G}_i^*$ is combined with a delay D of N_D samples in order to ensure that $D\overline{G}_i^*$ is predominantly causal. The transfer function G_{rp} subtracts the contribution of the actuators on the reference signals, as required for internal model control (IMC) [22].

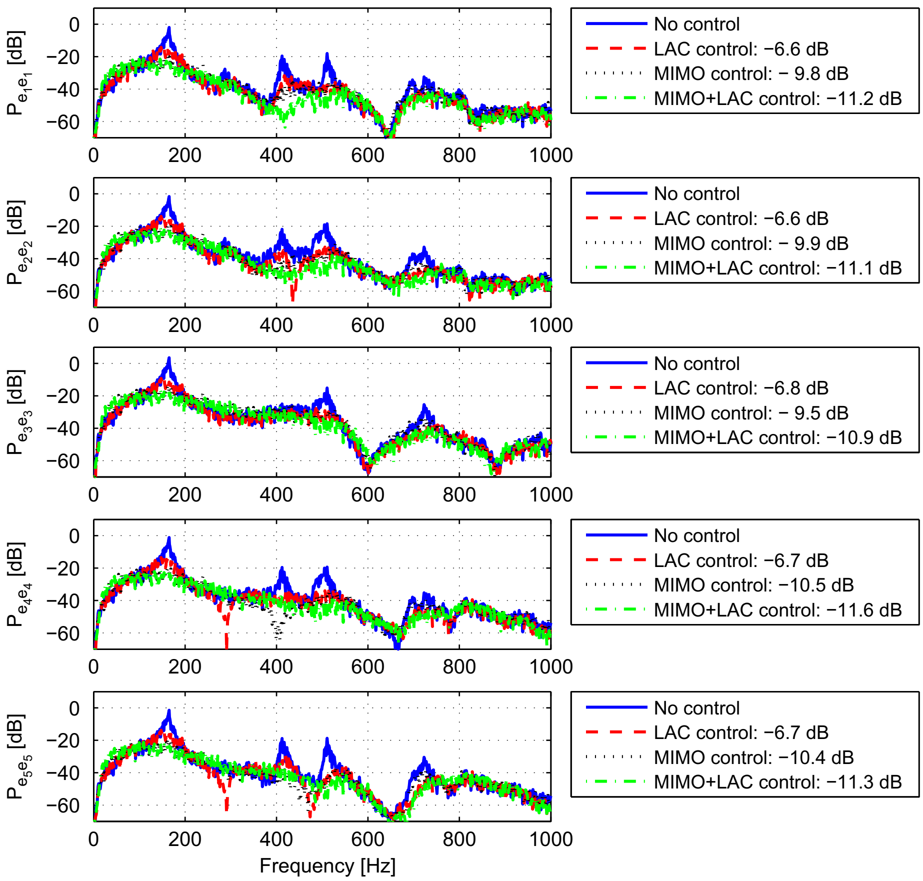

Fig. 10. Performance measured on the sensors for a feedback controller using IMC.

3. Results

3.1. Influence of LAC on the secondary path

For the idealized low-authority controller having the purpose to add damping to the system the phase should be between -90° and $+90^\circ$ for each collocated pair. Figs. 6 and 7 can be used to judge the practical setup involving the piezoelectric patch actuator and the accelerometer regarding this requirement. In Fig. 6, it can be seen that for frequencies up to 1 kHz the phase is between 0° and $+180^\circ$. Thus, with an integrator the phase will be between -90 and $+90^\circ$. In Fig. 7, it can be seen that for higher frequencies the phase lag is larger. Based on these results, the decentralized controllers were configured with an integrator and a first-order roll-off above 1 kHz. The gain was adjusted in such a way that a gain margin of at least 6 dB was obtained for each collocated pair, resulting in a maximum feedback gain of 64. For lower feedback gains the gain margin was higher. Significant cross-talk exists between the non-collocated pairs, which for some frequencies can be as large as the transfer function between the collocated pairs. The results confirm that if the actuator and sensor are located at the same place and are energetically conjugated, or approximately as in this paper, then the controller can be implemented in a decentralized manner [11,19]. The influence of LAC on HAC is taken into account in the system identification for HAC. The influence of LAC on the measured transfer function for HAC is shown in Fig. 8. It can be seen that resonances and antiresonances can be damped, particularly at low frequencies. For higher frequencies and for higher feedback gains some spillover can be observed. For this particular configuration also a controller configuration was tested in which the center actuator–sensor pair had a higher gain than the other pairs (see Fig. 8). Among the configurations studied, this configuration was found to give the best compromise between damping performance and spillover.

3.2. Selection of the convergence coefficient

In order to select a suitable value of the convergence coefficient α, the influence of α on the convergence speed and the MSE was studied by measuring the error signals for a duration of 60 s. At the beginning of each measurement the

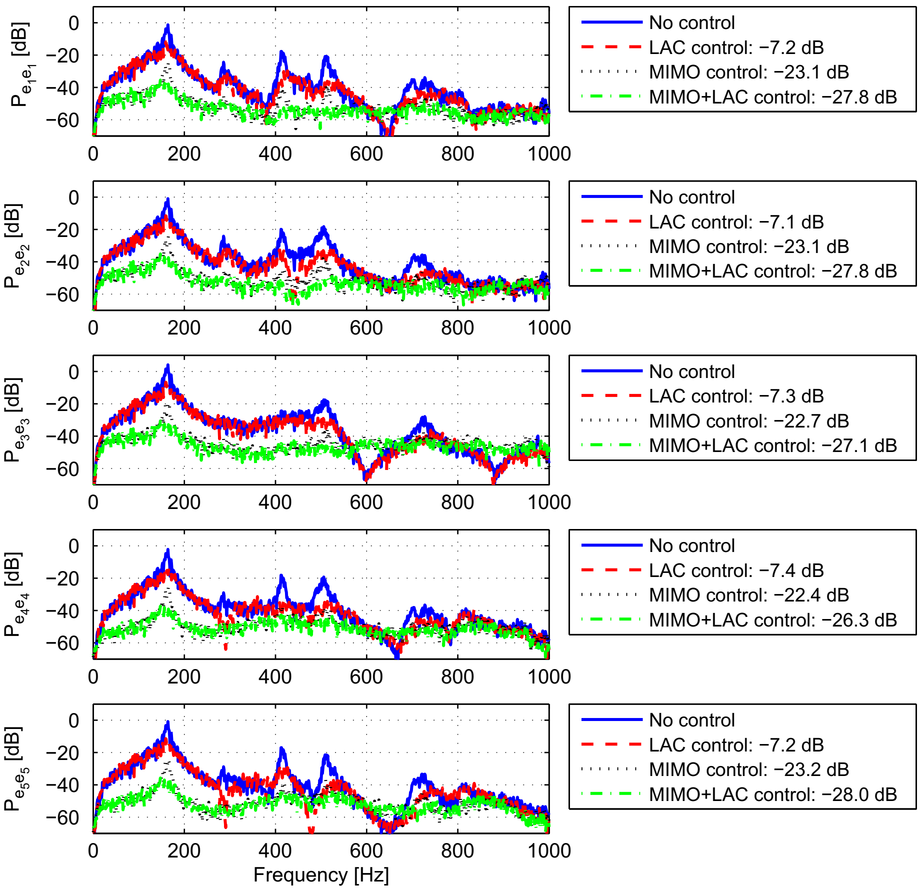

Fig. 11. Performance of the feedforward controller.

controller was switched off for 5 s and then it was switched on for 55 s. The reduction was calculated by taking the first 4 s and the last 4 s, using ensemble averages based on 32 measurements. For the feedback controller the following parameters were used: N_W=80, N_D=80, $\gamma = 10^{-5}$, in which γ sets the amount of leakage [10] of the control coefficients. The regularization parameter β was set to -20 dB. In Table 1, the result for a number of different step sizes α is given. A plot of the different convergence curves is not included due to the fact that the curves were almost identical: only the MSE errors were different. From Table 1, it can be concluded that $\alpha = \frac{1}{40}$ gives the best possible reduction after 60 s.

For the feedforward controller, the following parameters were used: N_W=350, N_D=80, $\gamma = 10^{-5}$. The regularization parameter β was set to -30 dB. The procedure used to measure the results for feedforward control was the same as used in the feedback scenario described in the previous paragraph, this time using 16 measurements. The different MSE values after convergence for different values of α can be found in Table 2. The convergence curves for different values of α can be found in Fig. 9. From these results, it was concluded that an α of $\frac{1}{40}$ was a good trade-off between convergence speed and steady-state MSE for HAC.

3.3. Influence of LAC on the steady-state mean-square error

Control results for a HAC/LAC architecture using an adaptive MIMO *feedback* algorithm are shown in Fig. 10. The convergence coefficient was set to $\alpha = \frac{1}{40}$ (see Section 3.2). It can be seen that the reduction of the error signals for MIMO control (HAC) is higher than for the decentralized control (LAC). The combination of HAC and LAC leads to the largest reduction of the error signals. The average improvement by adding the low-authority controller to the high-authority controller is approximately 1.4 dB.

Control results for a HAC/LAC architecture using an adaptive MIMO *feedforward* algorithm are shown in Fig. 11. The convergence coefficient was set to $\alpha = \frac{1}{40}$ (see Section 3.2). It can be seen that the reduction of the error signals for MIMO control (HAC) is considerably higher than for the decentralized control (LAC). As with feedback control the combination of HAC and LAC leads to the largest reduction of the error signals. The average improvement by adding the low-authority controller to the high-authority controller is approximately 4.4 dB.

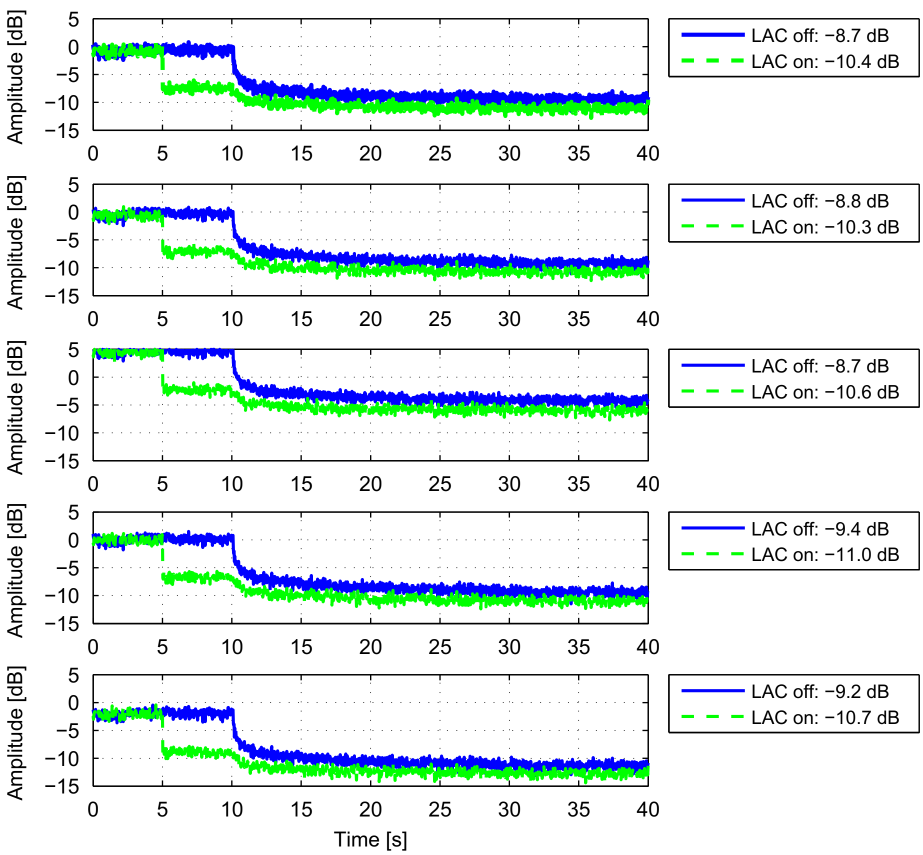

Fig. 12. Convergence curves for MIMO feedback with and without LAC.

Please cite this article as: A.P. Berkhoff, J.M. Wesselink, Combined MIMO adaptive and decentralized controllers for broadband active noise and vibration control, Mechanical Systems and Signal Processing (2011), doi:10.1016/j.ymssp.2010.12.012

3.4. Influence of LAC on the convergence speed

The objective was to find out how LAC influences the overall performance in terms of speed of convergence. Based on Section 3.2 it was decided to set α to a value of $\frac{1}{40}$ for the feedback controller as well as for the feedforward controller. The convergence under influence of LAC using a feedback HAC strategy can be found in Fig. 12. To show the impact of the LAC clearly, it was decided to leave the LAC switched off for the first 5 s and switched on for the remainder of the time. The two plots in Fig. 12 demonstrate the difference between a high-authority controller with and without LAC. The plots show that LAC does not significantly influence the speed of convergence. However, the MSE improves with approximately 1.5–2 dB.

The same experiment was also carried out for the feedforward HAC algorithm. In this scenario, the reference signal was directly taken from the noise generator. The results of this measurement can be found in Fig. 13. In this scenario, the LAC unit was again switched off for the first 5 s and then switched on for the remainder of the duration. It can be concluded that the LAC unit does not influence the speed of convergence. However, it does improve the MSE by approximately 5 dB.

For both feedback HAC and feedforward HAC, LAC does not modify the speed of convergence. Apparently, the preconditioning part of the RMFeLMS algorithm, which is designed to remove the eigenvalue spread of the autocorrelation matrix of the filtered-reference signal [10], works as expected since LAC has a significant influence on this eigenvalue spread.

3.5. Influence of LAC on the robustness

A subsequent set of tests was performed to study the influence of LAC on the robustness of the controller. The robustness was evaluated by adding different weights to the panel. The high-authority controller for these tests was based on a model that was obtained without the additional weight. Fig. 14 shows the phase difference between the situations with added mass and without added mass of the models as identified for the high-authority controller for the cases that the low-authority controller was switched on and for the case that the low-authority controller was switched off. In this figure, it can be seen that for low frequencies the system is less sensitive to the addition of mass when the low-authority controller is switched on. Therefore, it was expected that the robustness of the present high-authority controller would

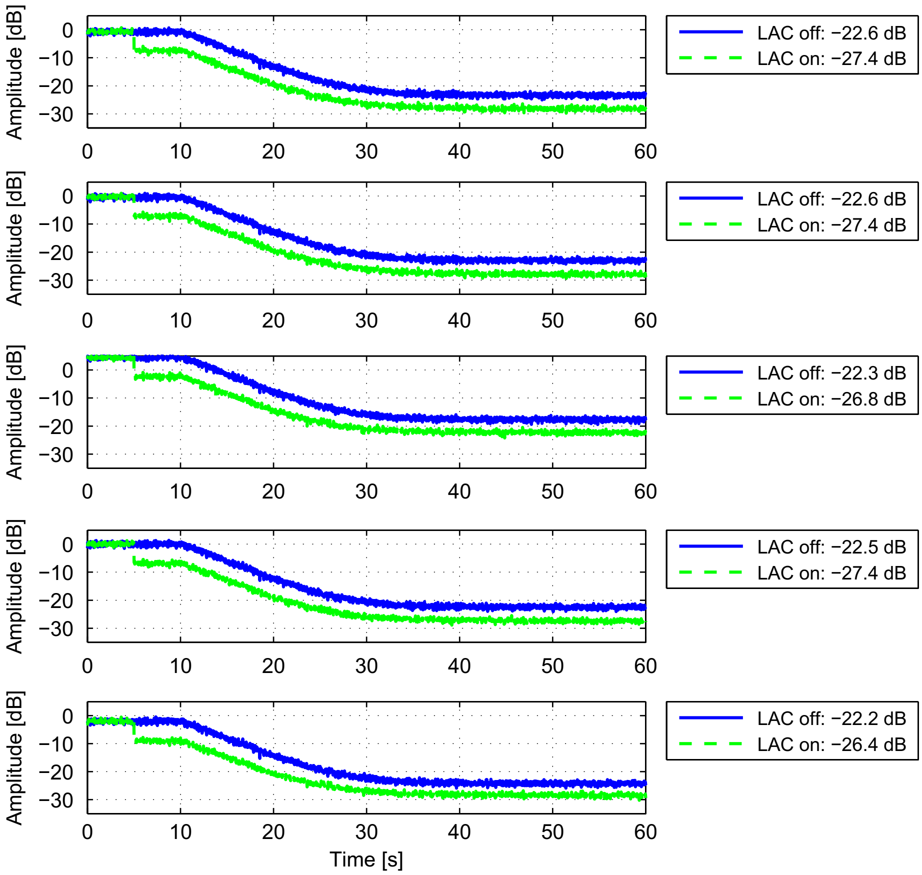

Fig. 13. Convergence curves for MIMO feedforward control with and without LAC.

Please cite this article as: A.P. Berkhoff, J.M. Wesselink, Combined MIMO adaptive and decentralized controllers for broadband active noise and vibration control, Mechanical Systems and Signal Processing (2011), doi:10.1016/j.ymssp.2010.12.012

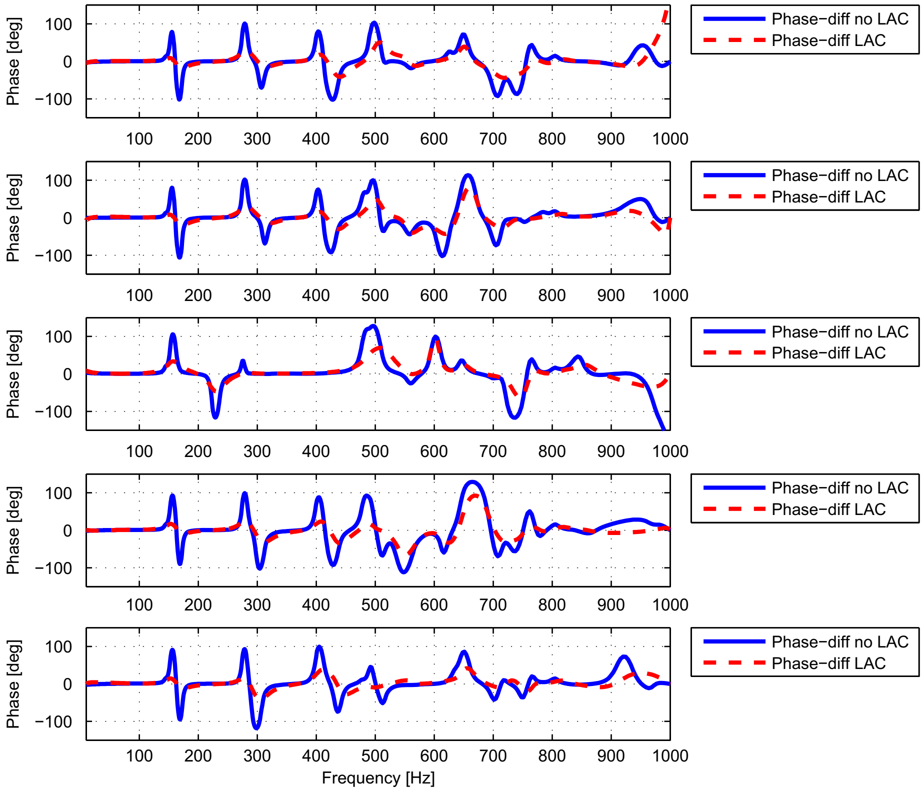

Fig. 14. A plot of the phase difference between systems with and without additional weight. The first curve uses no LAC and the second one has LAC enabled. In this case a weight of 40.60 g was added to the panel.

Table 3
Influence of added weight on the performance of a feedback controller. The reduction was measured after 180 s and was the average MSE reduction in dB over all five sensors. A step size $\alpha = \frac{1}{40}$ was used. The model for IMC and the RMFeLMS algorithm were identified without the additional weight.

Weight (g)	MSE reduction (dB)					
	$\beta = -20$ dB		$\beta = -25$ dB		$\beta = -30$ dB	
	LAC on	LAC off	LAC on	LAC off	LAC on	LAC off
00.00	11.4	10.4	12.0	10.5	12.1	11.8
18.17	11.5	10.4	12.4	10.9	13.0	11.6
27.00	11.6	10.3	12.5	11.0	12.4	11.3
33.82	11.6	10.4	12.7	11.2	12.8	11.6
40.60	12.2	–	11.8	–	12.8	–
47.32	11.5	–	11.8	–	–	–
54.17	12.2	–	12.4	–	–	–
61.05	11.5	–	12.3	–	–	–
67.85	12.0	–	12.7	–	–	–
74.96	11.9	–	12.0	–	–	–
81.67	11.8	–	12.2	–	–	–
88.41	11.7	–	12.6	–	–	–
95.22	11.9	–	–	–	–	–

benefit from the addition of the low-authority controller since the robustness of the adaptive high-authority controller is primarily determined by the phase of the secondary path [10].

Indeed, the robustness of the adaptive controllers improved by the addition of the low-authority controller. The results for the robustness of the adaptive feedback controller are summarized in Table 3. This table contains the average reductions of the error signals provided the system was stable. The reductions are given for different values of added weight as well as different values of the regularization of the controller. It can be seen from the results in this table that, firstly, larger weights can be added if LAC is switched on, and therefore, the robustness improves by the addition of LAC,

Table 4
Influence of added weight on the performance of a feedforward controller. The performance was measured after 180 s. A step size $\alpha = \frac{1}{40}$ was used. The model for the RMFeLMS algorithm was identified without additional weight.

Weight (g)	MSE reduction (dB)					
	$\beta = -25$ dB		$\beta = -30$ dB		$\beta = -35$ dB	
	LAC on	LAC off	LAC on	LAC off	LAC on	LAC off
00.00	25.4	21.4	27.5	22.2	27.6	22.6
18.17	25.3	21.6	26.9	21.5	28.7	22.8
27.00	24.7	–	26.2	–	27.3	–
33.82	25.2	–	22.6	–	–	–
40.60	–	–	–	–	–	–

Table 5
Influence of added weight on the performance of a feedback controller. The performance was measured after 180 s. A step size $\alpha = \frac{1}{40}$ was used. In this case the LAC unit was switched off but the model used LAC and was used for IMC and the RMFeLMS controller. This model was identified without additional weight but with LAC switched on. The regularization level β was set to -25 dB.

Weight (g)	00.00	18.17	27.00	33.82	40.60	47.32	54.17	61.05	67.85
MSE reduction (dB)	11.3	11.7	11.9	11.6	11.7	11.4	11.4	11.5	–

secondly, that higher levels of the regularization parameter β also lead to increased robustness, and thirdly, for low values of β the improvement by LAC is marginal. Furthermore, the regularization by β does not seem to influence the robustness if LAC is switched off. Especially for regularization levels of $\beta = -20$ dB and -25 dB there is a significant improvement of the robustness by the addition of LAC. Similar results can be found for the feedforward controller, as shown in Table 4, although in this case the emphasis of the improvement is on the reduction of the mean-square value of the error signal instead of the robustness. The relative importance of the robustness and the reduction of the mean-square error is influenced by the value of the regularization level β, which was not equal for the feedforward controller and the feedback controller. The regularization level for the feedback controller was set to a somewhat higher level than for the feedforward controller. One reason is that, on the one-hand, it does not make sense to use an extremely small regularization level for feedback controllers since it will not reduce the mean-square error anymore. On the other hand, if the value of the regularization level is set too high for the feedforward controller then the performance gain of the feedforward controller over the feedback controller is relatively small.

An interesting observation was that the robustness of the adaptive feedback controller also increased if the model was obtained with LAC switched on but for which, during control operation, the LAC was switched off. The results of these tests can be found in Table 5. Apparently, the reduced phase in the model itself is beneficial for the robustness of the controller. This suggests that the addition of numerical damping to the a-priori determined transfer functions would lead to improved robustness. By doing so one could obtain more robust controllers without an additional effort of implementing the decentralized controllers. One technique to realize the numerical damping is to apply an LQR regulator [6] to the identified plant and set the weighting matrices in such a way that the desired amount of damping is obtained. Alternatively, if the plant contains significant phase delays, one could add damping to the minimum-phase factor of the plant. Nevertheless, it was found that the full HAC-LAC control strategy resulted in the best performance and robustness properties.

4. Conclusion

In this paper, real-time results were shown of a combination of fixed decentralized feedback control (low-authority control) with multiple-input multiple-output adaptive control (high-authority control). The system was applied to a panel with piezoelectric actuators, piezoelectric sensors, and acceleration sensors. The HAC/LAC architecture was realized as a high-speed decentralized controller on a field programmable gate array (FPGA) and a medium speed centralized controller on a central processing unit (CPU). For the configurations that were studied, the increase in robustness was most noticeable for an adaptive feedback controller, whereas, for the adaptive feedforward controller, the improvement of performance was most noticeable with respect to the reduction of the mean-square value of the error signals.

It was found that low-authority control has no significant influence on the speed of convergence of the high-authority controller as used in this paper, both for feedback and feedforward configurations.

It was also shown that secondary path models with added damping, as obtained with low-authority control, can lead to improved robustness even if high-authority feedback control is used without low-authority control. This suggests that artificially added damping, which could be added numerically to the models obtained from system identification, can lead to improved robustness properties.

Please cite this article as: A.P. Berkhoff, J.M. Wesselink, Combined MIMO adaptive and decentralized controllers for broadband active noise and vibration control, Mechanical Systems and Signal Processing (2011), doi:10.1016/j.ymssp.2010.12.012

Acknowledgments

The authors would like to thank Geert Jan Laanstra and Henny Kuipers of University of Twente, Signals and Systems group, Faculty EEMCS for the excellent support. Part of this work was performed within the EU-FP6 project Intelligent Materials for Active Noise Reduction (InMAR).

References

[1] S.M. Kuo, R.D. Morgan, Active Noise Control Systems, John Wiley & Sons Inc., USA, 1996.
[2] S.J. Elliott, Optimal controllers and adaptive controllers for multichannel feedforward control of stochastic disturbances, IEEE Transactions on Signal Processing 48 (2000) 1053–1060.
[3] E.A. Wan, Adjoint LMS: an efficient alternative to the filtered-X LMS and multiple error LMS algorithms, in: ICASSP, IEEE International Conference on Acoustics, Speech and Signal Processing—Proceedings, IEEE, Piscataway, NJ, USA1996, pp. 1842–1845.
[4] J.M. Wesselink, A.P. Berkhoff, Fast affine projections and the regularized modified filtered-error algorithm in multichannel active noise control, The Journal of the Acoustical Society of America 124 (2008) 949–960.
[5] S.J. Elliott, Adaptive methods in active control, in: M.O. Tokhi, S.M. Veres (Eds.), Active Sound and Vibration Control, IET, London, pp. 57–72 (Chapter 3).
[6] K. Zhou, J.C. Doyle, K. Glover, Robust and Optimal Control, Prentice-Hall, Upper Saddle River, NJ, 1996.
[7] M. Sternad, A. Ahlen, Robust filtering and feedforward control based on probabilistic descriptions of model errors, Automatica 29 (1993) 661–679.
[8] B. Bernhardsson, Robust performance optimization of open loop type problems using models from standard identification, Systems and Control Letters 25 (1995) 79–87.
[9] B. Rafaely, S.J. Elliott, A computationally efficient frequency-domain LMS algorithm with constraints on the adaptive filter, IEEE Transactions on Signal Processing 48 (2000) 1649–1655.
[10] S.J. Elliott, Signal Processing for Active Control, Academic Press, London, 2001.
[11] A. Preumont, Vibration Control of Active Structures, second ed., Kluwer Academic Publishers, Dordrecht, 2002.
[12] S. Herold, D. Mayer, H. Hanselka, Transient simulation of adaptive structures, Journal of Intelligent Material Systems and Structures 15 (2004) 215–224.
[13] S.J. Elliott, P. Gardonio, T.C. Sors, M.J. Brennan, Active vibroacoustic control with multiple local feedback loops, Journal of the Acoustical Society of America 111 (2002) 908–915.
[14] A.P. Berkhoff, G. Nijsse, A rapidly converging filtered-error algorithm for multichannel active noise control, International Journal of Adaptive Control and Signal Processing 21 (2007) 556–569.
[15] P.V. Overschee, B.D. Moor, Subspace Identification for Linear Systems, Kluwer Academic Publishers, Dordrecht, The Netherlands, 1996.
[16] M. Vidyasagar, Control System Synthesis: A Factorization Approach, MIT Press, Boston, 1985.
[17] V. Ionescu, C. Oara, M. Weiss, Generalised Riccati Theory and Robust Control: A Popov Function Approach, John Wiley & Sons Ltd, Chichester, England, 1999.
[18] A.P. Berkhoff, Weight reduction and transmission loss tradeoffs for active/passive panels with miniaturized electronics, in: R.H. Cabell, G.C. Maling (Eds.), Proceedings of Active 04, INCE USA, Washington, DC2004, pp. 1–12.
[19] P. Gardonio, E. Bianchi, S.J. Elliott, Smart panel with multiple decentralized units for the control of sound transmission. Part I: theoretical predictions, Journal of Sound and Vibration 274 (2004) 163–192.
[20] P. Gardonio, E. Bianchi, S.J. Elliott, Smart panel with multiple decentralized units for the control of sound transmission. Part II: design of the decentralized control units, Journal of Sound and Vibration 274 (2004) 193–213.
[21] E. Bianchi, P. Gardonio, S.J. Elliott, Smart panel with multiple decentralized units for the control of sound transmission. Part III: control system implementation, Journal of Sound and Vibration 274 (2004) 215–232.
[22] M. Morari, E. Zafiriou, Robust Process Control, Prentice-Hall, London, 1989.